科技资料

Infrared Imaging Systems: Design, Analysis, Modeling, and Testing II

PROCEEDINGS
SPIE—The International Society for Optical Engineering

Infrared Imaging Systems: Design, Analysis, Modeling, and Testing II

Gerald C. Holst
Chair/Editor

3-5 April 1991
Orlando, Florida

Sponsored and Published by
SPIE—The International Society for Optical Engineering

Cooperating Organization
CREOL/University of Central Florida

Volume 1488

The papers appearing in this book comprise the proceedings of the meeting mentioned on the cover and title page. They reflect the authors' opinions and are published as presented and without change, in the interests of timely dissemination. Their inclusion in this publication does not necessarily constitute endorsement by the editors or by SPIE.

Please use the following format to cite material from this book:
Author(s), "Title of paper," *Infrared Imaging Systems: Design, Analysis, Modeling, and Testing II,* Gerald C. Holst, Editor, Proc. SPIE 1488, page numbers (1991).

Library of Congress Catalog Card No. 90-52794
ISBN 0-8194-0597-3

Published by
SPIE—The International Society for Optical Engineering
P.O. Box 10, Bellingham, Washington 98227-0010 USA
Telephone 206/676-3290 (Pacific Time) • Fax 206/647-1445

Printed in the United States of America

INFRARED IMAGING SYSTEMS:
DESIGN, ANALYSIS, MODELING, AND TESTING II

Volume 1488

CONFERENCE COMMITTEE

Conference Chair

Gerald C. Holst, Martin Marietta Electronic Systems Center

Cochairs

John A. D'Agostino, U.S. Army Center for Night Vision and Electro-Optics
Paul J. Jennison, Spar Aerospace Ltd. (Canada)
Stephen W. McHugh, Santa Barbara Infrared, Inc.
James Ratches, U.S. Army Center for Night Vision and Electro-Optics
Philip H. Stahl, Rose-Hulman Institute of Technology

Session Chairs

Session 1—Poster Session

Session 2—Infrared System Analysis and Modeling I
Gerald C. Holst, Martin Marietta Electronic Systems Center

Session 3—Infrared System Analysis and Modeling II
James Ratches, U.S. Army Center for Night Vision and Electro-Optics

Session 4—Infrared System Analysis and Modeling III
John A. D'Agostino, U.S. Army Center for Night Vision and Electro-Optics

Session 5—Infrared System Analysis and Modeling IV
Philip H. Stahl, Rose-Hulman Institute of Technology

Session 6—Engineering Problems and Solutions Workshop
Gerald C. Holst, Martin Marietta Electronic Systems Center

Session 7—Infrared System Testing
Stephen W. McHugh, Santa Barbara Infrared, Inc.

Session 8—Infrared System Design
Paul J. Jennison, Spar Aerospace Ltd. (Canada)

Session 9—SPRITE Detectors
Paul J. Jennison, Spar Aerospace Ltd. (Canada)

Conference 1488, *Infrared Imaging Systems: Design, Analysis, Modeling, and Testing II*, was part of a three-conference program on Infrared Imaging Systems Analysis, held at the SPIE Symposium on Optical Engineering and Photonics in Aerospace Sensing, 1-5 April 1991, in Orlando, Florida. The other conferences were:

Conference 1486, *Characterization, Propagation, and Simulation of Sources and Backgrounds*
Conference 1487, *Propagation Engineering: Fourth in a Series*

Program Chair: **Walter B. Miller,** U.S. Army Atmospheric Sciences Lab.

INFRARED IMAGING SYSTEMS:
DESIGN, ANALYSIS, MODELING, AND TESTING II

Volume 1488

INTRODUCTION

Effective infrared system design, analysis, modeling, and testing cannot be performed effectively without detailed knowledge of the target-background signature and the atmospheric propagation parameters. This year, the Infrared Imaging Systems Analysis program consisted of three conferences: Conference 1486 (Characterization, Propagation, and Simulation of Sources and Backgrounds), Conference 1487 (Propagation Engineering: Fourth in a Series), and this one, Conference 1488.

This conference focused on system issues and consisted of 35 papers presented at seven sessions. Both a Poster Session and an Engineering Problems and Solutions Workshop were held jointly with Conferences 1486 and 1487.

The keen interest in second-generation FLIRs was evidenced by the number of papers presented in this area and by the large attendance. These systems have created new areas of research. Receiving much interest was the three-dimensional noise model presented by D'Agostino and Webb. For total system modeling, many of the models, such as the MISSPM (presented by Owen), contain the new C^2NVEO FLIR90 model (presented by Scott). Harold Kennedy highlighted the MTFs used in these models. Sampling effects are now considered major image modifiers (papers presented by Rogne, Holst, Rahman et al., and Warren et al.).

Eight papers were presented on infrared testing, and five on novel designs. Due to the current interest in SPRITE detectors, a separate session was held with four papers presented.

It was a pleasure to see so many outstanding papers presented at this conference. The question-and-answer period after each paper was lively and interesting. Informal discussions were held during the coffee breaks, at lunch, and continued at the end of each day.

I sincerely thank all the authors for their contributions and hard work. The conference was successful due to the efforts of the cochairs, John A. D'Agostino, Paul J. Jennison, Stephen W. McHugh, James Ratches, and Philip H. Stahl. I acknowledge their efforts and express my sincere appreciation to all of them.

Gerald C. Holst
Martin Marietta Electronics Systems Center

INFRARED IMAGING SYSTEMS:
DESIGN, ANALYSIS, MODELING, AND TESTING II

Volume 1488

CONTENTS

(continued)

INFRARED IMAGING SYSTEMS:
DESIGN, ANALYSIS, MODELING, AND TESTING II

Volume 1488

INFRARED IMAGING SYSTEMS:
DESIGN, ANALYSIS, MODELING, AND TESTING II

Volume 1488

SESSION 1

Poster Session

New type IR to visible real—time image converter: design and fabrication

Fang—kui Sun, Mao—hua Yang, Shao—hong Gao, and Shi—jie Zhao

Dept. of Applied Physics, Harbin Institute of Technology, Harbin, China, 150006

ABSTRACT

This paper introduces the design principle of a new type of IR to visible real—time image converter and the general process of its fabrication. The analysis indicates that the improvement of the device performance is closely linked with the match among various parameters.

1. INTRODUCTION

Since the first photo—electric camera tube was invented in the 1930s, many kinds of IR to visible photo—electric camera tubes have been developed. The sensitivity, resolution and other parameters of these camera devices which are based on electron beam scanning have reached a high standard. However, at present there is no report about the development of the converter which can turn an IR image to a visible one directly without using electric transducing treatment.

This paper reports for the first time about the design and fabrication of an IR to a visible real—time image converter. This drvice is a new type of photoelectric one which is based on liquid crystal modulation. [1]In the course of the device development, the primary measurement shows that the device can be safely put into practical application. The main parameters of the device are expected to reach:

1. the resolution is larger than 30lp/mm (the limit resolution)
2. the contrast ratio is 100 : 1
3. the response time is μs.

This device is expected to be applied in the fields of aviation night vision and sea survey, etc.

2. STRUCTURE DESIGN

This device is mainly composed of some kinds of films which are plated between two glass base slices. Among the films, the key ones are the liquid crystal film and the photoconductive film. The basic structure of the device is shown in Fig. 1. Fig. 1(6)can both attenuate and resist IR rays and reflect the read light on the other side. Thus, the device can write and read out at the same time without considering the composition of spectrums of light beams.

3. WORKING PRINCIPLE

The equivalent circuit of the device is shown as Fig. 2 in which Vb is an applied alternating audio—frequency power, Rp and Cp stand for the resistance and the capacity of the IR photosensitive layer respectively; and R_l and C_l stand for the resistance and the capacity of the liquid crystal layer respectively. The impedances of other films are much less than the above and could be neglected completely.

According to Fig. 2, the change of R_p will cause the corresponding change of voltage between both ends of the liquid crystal layer and thus serves as an optically controlled voltage.

When the device is at work, IR images first pass through the optical filter layer 10(see Fig. 1)for wave filtering, then go through IR glass 9 and IR transparant electrode 8, and finally irradiate on IR sensitive layer 7. After that, the specific conductance of the sensitive layer changes in varying degrees in accordance with the irradiation intensity, that is,

 0-8194-0597-3/91/$4.00

R_p in Fig. 2 will vary. According to Fig. 2, the voltage between both ends of the liquid crystal laver will vary in accordance with the impedance of the IR photosensitive layer. According to the mixed field effect theory of nematic liquid crystal,[2] the twist angle and the inclined angle of the molecules in the liquid crystal will change in varying degrees. When we read with visible line polarized lights from the other side, the visible line polarized lights coming through the liquid crystal layer will produce birefringence effects in varying degrees. Thus the polarized direction of the lights reflected from resisting layer 6 is consistant with the irradiation grey scale of IR image. After going through a vertical polarization analyzer, the read lights show the irradiating images real—timely. Therefore, the IR to visible real—time image conversion is achieved.

4. FABRICATION AND MATCH

In the fabrications of the device, the preparations of the IR photoconductive film and the liquid crystal layer are more important, while the other films preparation can depend on conventional and skilled technology. In the device, the liquid crystal of 45^0 twist angle is used, because under reflection, it may produce maximum birefringence effect, besides, it has a larger dynamic range together with a higher output intensity. According to the modulation features to rays under different voltages and frequencies, the proper selecting of a working voltage and an alternating frequency is an important step.

Because the alternating resistivity magnitude of the liquid crystal is about $10^{10}\Omega \cdot cm$, the dark resistivity of PbSe plated photoconductive film must be larger than $10^9\Omega \cdot cm$ in order to match the alternating resistivity.

The photoconductive film PbSe produced by vaporing and illuviating directiy has a lower dark resistivity and poor photoconductivity, because during vaporing, Pb and Se have different vapor tensions whic causes the proportion of Pb to Se in the illuviating film to exceed the stoichiometric proportion of Pb to Se in PbSe. Thus the treatment of high temperature annealing and doping must be used to remove or fuse the additional Pb and then to make acceptor impurity permeating. In this paper, a different treatment from usual methods is used, and the high temperature annealing and doping Cu for sensitization in a constant temperature furnace is adopter. The powdered Cu will stick to the PbSe film closely under a high temperature (400^0c, heating—up time being 0.5——4hr) and come into it by means of the thermal diffusion. The experiment proves that the strict controlling of the technological parameters and the stabilizing of the experimental condition is of vital importance to the obtaining of high—quality photoconductive films; while the excess of doping density, heating—up temperature and time would decrease the dark resistivity and the photosensitivity of photoconductive films as well.

In Fig. 2, each $1cm^2$ film layer is measued with a precise bridge and obtained: $R_l = 10^8\Omega$, $C_l = 800PF$; while in a dark atate $R_p = 5.3 \times 10^9\Omega$, $C_p = 900PF$; when the light intensity equals $150\mu w/cm^2$, $R_p = 2.6 \times 10^9\Omega$, $C_p = 3600PF$. These results show that with direct impedance, the equivalent resistance of the liquid crystal layer is several ten times as small as that of the heterojunction. Thus, if lower working voltage frequency is selected, the device could not work because of the impedance unmatching between the liquid crystal and the photoconductive film. On the contrary, if a higher working voltage frequency is selected, the capacity current of the device would play the dominant role and the matching would be easily achieved. However, an excessive working frequency may decrease the dark—to—bright impedance ratio of the photoconductive film, and therefore decrease the resolution of the device. The experiment shows that it is most appropriate to adopt the alternating working frequency about about $2KH_z$, The measurement of the performance parameters of the liquid crystal layer indicates that when the alternating voltage of the liquid crystal layer ranges within 20—25V, the contrast ratio of light intensity could get 100 : 1, and that the impedance changing caused by the irradiation intensity of IR images may cause the changing range of the alternating voltage of the liquid crystal layer to cover the area completely. Therefore, the impedance matching between the liquid crystal layer and the photoconductive film is achieved.

The response rate of the device depends on the response times of the liquid crystal and photoconductive film as well as the impedance matching of films. In this paper, the ferroelectric liquid crystal whose response time is μs magnitude and PbSe

whose response time is less than 5μs are adopted to achieve this requirement.

5. REFERENCES

1. J. Gringberg, et al. , Opt. ,ED—22,775(1975)
2. Anthony M. Tai, Appl. Opt. ,25,9,1380(1986)
3. J. D. Margerum, et al. ,Appl. Phys. Lett. ,17,51(1970)
4. K. W. Boer, et al. ,J. Appl. Phys. ,37,7,2664(1966)

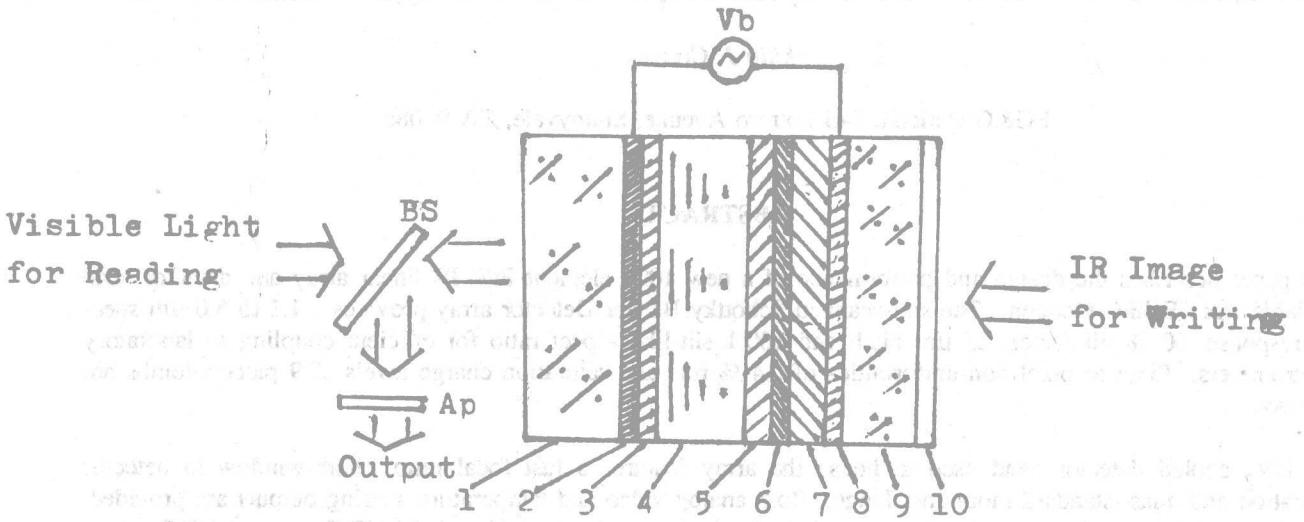

Fig.1. Basic structure of the device (sectional view)

1--- common glass; 2, 8--- transparant electrode;
3, 5--- S_iO_2 directional film; 4--- liquid crystal;
6--- IR resist-light layer; 7--- IR sensitive layer;
9--- IR glass; 10--- filter layer.

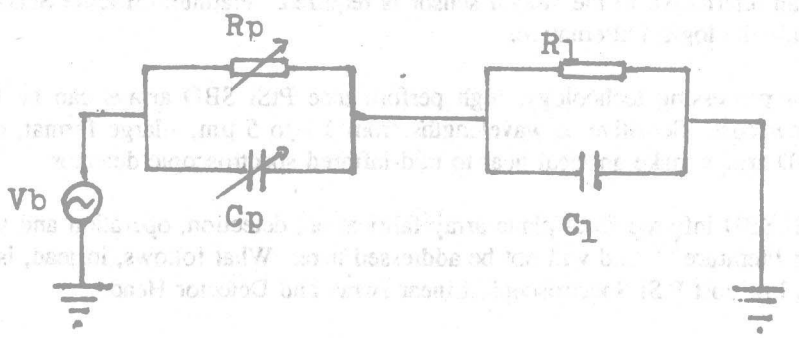

Fig.2. Equivalent circuit of the device

Design and Performance of a PtSi Spectroscopic Infrared Array and Detector Head

Philip J. Cizdziel

EG&G Reticon, 345 Potrero Avenue, Sunnyvale, CA 94086

ABSTRACT

This paper describes the design and performance of a new 1024 element PtSi IR linear array and detector head available from EG&G Reticon. The self-scanned Schottky Barrier Detector array provides a 1.1 to 5.0 μm spectral response, 60 % fill factor, 25 μm pitch and 100:1 slit-like aspect ratio for efficient coupling to laboratory spectrometers. Pixel to pixel non-uniformities of 0.4 % rms and saturation charge levels of 9 picocoulombs are achieved.

The LN_2 cooled detector head used to house the array features a fast focal ratio, short window to detector separation and quasi-standard mounting flange. Both analog video and temperature sensing outputs are provided. Timing may be internally or externally controlled. In the former mode, only +/- 15 VDC and + 5 VDC power inputs are needed. In the latter mode, external clock and sync inputs as well as power are required.

The sensor, dewar and coldshielding is described; as well as the analog, digital and temperature sensing electronics. A discussion of system-wide performance data and technical specifications concludes the review.

1. INTRODUCTION

Silicon CCDs and photodiode arrays have been used successfully for spectroscopic observations from the UV to the near IR by physicists, astronomers and chemists for years. Because of the 1.12 eV bandgap of silicon however, all such observations have been limited to electromagnetic wavelengths short of 1.1 μm.

Unfortunately, the telltale spectral features of many neutral and ionized atomic species, as well as the vibration-rotation bands of numerous important molecules lie at infrared wavelengths beyond 1.1 μm. In order to study such spectral features, an alternative to the silicon sensor is required. Platinum-Silicide Schottky Barrier Diode (PtSi SBD) arrays provide the logical alternative.

Compatible with silicon processing technology, high performance PtSi SBD arrays can be fabricated in large numbers at relatively low cost. Sensitive to wavelengths from 1.1 to 5 μm, --large format, cosmetically clean, highly uniform PtSi SBD arrays make an ideal near to mid-infrared spectroscopic detector.

The basic theory of PtSi SBD infrared focal plane array fabrication, detection, operation and testing is thoroughly covered in the recent literature[1-5] and will not be addressed here. What follows, instead, is a description of a new, high performance, low cost PtSi Spectroscopic Linear Array and Detector Head.

The next section of this paper describes the Sensor Chip, while the following discusses the Detector Head Dewar, Optics and Cold Shielding. The Digital, Analog and Temperature Sensing circuit boards are briefly described in Section 4. Last but not least, Detector Head System Performance is presented in Section 5.

2. SENSOR CHIP

The photosensitive element in the Spectroscopic Detector Head is a backside illuminated, Platinum Silicide Schottky Barrier Diode (PtSi SBD) array. The center to center spacing of the pixels in the array is 25 μm, while the active area of each pixel is 15 μm x 2500 μm. This results in a 60% fill factor over a 1.00 x 0.10 inch active area. Note: (1) The 100:1 slit-like pixel-aspect-ratio makes for efficient coupling to laboratory spectrometers and (2) the array and detector head also come in a 512 element version identical in design and performance

 0-8194-0597-3/91/$4.00

to the 1024 element version described here.

The PtSi die is mounted in a 34 pin dual in-line ceramic package. Pixel 1 is located at the pin 1 end of the chip. To accomodate backside illumination and cryogenic cooling of the chip, a slot is placed in the top of the package, an opaque lid is glued to the bottom of the package and the leads are braised to the body in a direction opposite to that of a traditional dual in-line package. The pinout of the device is shown in Figure 1, while a simplified schematic is shown in Figure 2.

The 1024 element sensor chip consists of (1) a 1030-stage scanning shift register [6 dummy stages followed by 1024 active stages], (2) a 1024 element array of multiplexing switches and associated active PtSi SBDs, as well as a 1024 element array of multiplexing switches and associated dummy Si diodes, (3) two video output lines, one for the active diode readout and the other for dummy diode readout, (4) two video output transistors, one for active video reset and the other for dummy video reset and (5) two built-in silicon temperature sensing diodes (mounted on either end of the array). Note - The multiplexed dummy Si diodes (1) are much, much smaller than the multiplexed active PtSi SBDs, (2) are located on the periphery of the active area between the shift register and the PtSi SBDs, and (3) are not intended for photodetection. A large, unmultiplexed, dummy silicon diode is also attached to the dummy video line. This diode is 15 μm x 2500 μm in size, located at the pixel 1024 end of the chip, and (like its smaller counterparts) is intended to capacitively balance the dummy video line (and not to detect photons).

In operation, the scanning register sequentially enables one multiplexing gate at a time. Once enabled, photocharge flows off the active (and dummy) diodes and onto the appropriate video lines to be sensed at the output. Note - The two video output transistors mentioned above are not used in the present detector head configuration. Detector reset is performed by tieing each of the two video output lines to a +2.5 VDC virtual ground.

2.1 Spectral Response

The spectral response of a typical Reticon PtSi SBD is shown in Figures 3 and 4. The former displays Current Responsivity as a function of wavelength, while the latter displays Absolute Quantum Efficiency as a function of wavelength. Note: This data comes from a 15.5 mil square PtSi Schottky Barrier 'witness test diode' with a quarter-wave optical cavity peaked for 3.5 μm wavelength[6] and is believed to be an accurate indicator of array performance. A globar-illuminated, grating-monochrometer and specially coated and calibrated pyroelectric reference detector were used for this measurement.

At wavelengths beyond 2.5 μm, the data fits a PtSi SBD curve quite nicely, while at wavelengths shorter than 2.5 μm, the effects of the optical cavity (situated beyond the thin PtSi layer) and the absorption of radiation passing througth the silicon substrate (situated before the thin PtSi layer) are clearly evident[7]. Note the sharp dip in spectral response at 1.75 μm (=3.50 μm / 2) and the sharp drop in spectral response at 1.1 μm, respectively. Future PtSi spectroscopic arrays will be built with quarter-wave optical cavities peaked for 1.0 μm wavelength, eliminating the QE antinode from the 1 to 5 μm passband altogether.

The small non-zero response at wavelengths just under 1.1 μm is real and believed to be due to the absorption of IR photons in the silicon substrate near the junction. In fact, modeling the substrate as a semi-infinite slab and assuming unpolarized light at normal incidence, we find that 64% of the 1.00 μm light and 10% of the 0.95 μm light striking the backside of the 77°K, 21 mil thick silicon substrate reaches the junction[8,9].

The relatively low quantum efficiency of PtSi SBDs compared to silicon photodiodes of equal surface area stems from (1) the vastly different physics involved (the internal photoemission mechanism vs. the band to band transition mechanism) and (2) the much smaller collection volume of a PtSi SBD compared to a silicon photodiode.

In a silicon photodiode, charge carriers created by the absorption of a UV or visible wavelength photon in the depletion region (and up to a diffusion length away in the bulk silicon) are collected. In a PtSi SBD however, IR photons are only absorbed (hence photo-induced charge carriers are only created) in the very thin silicide

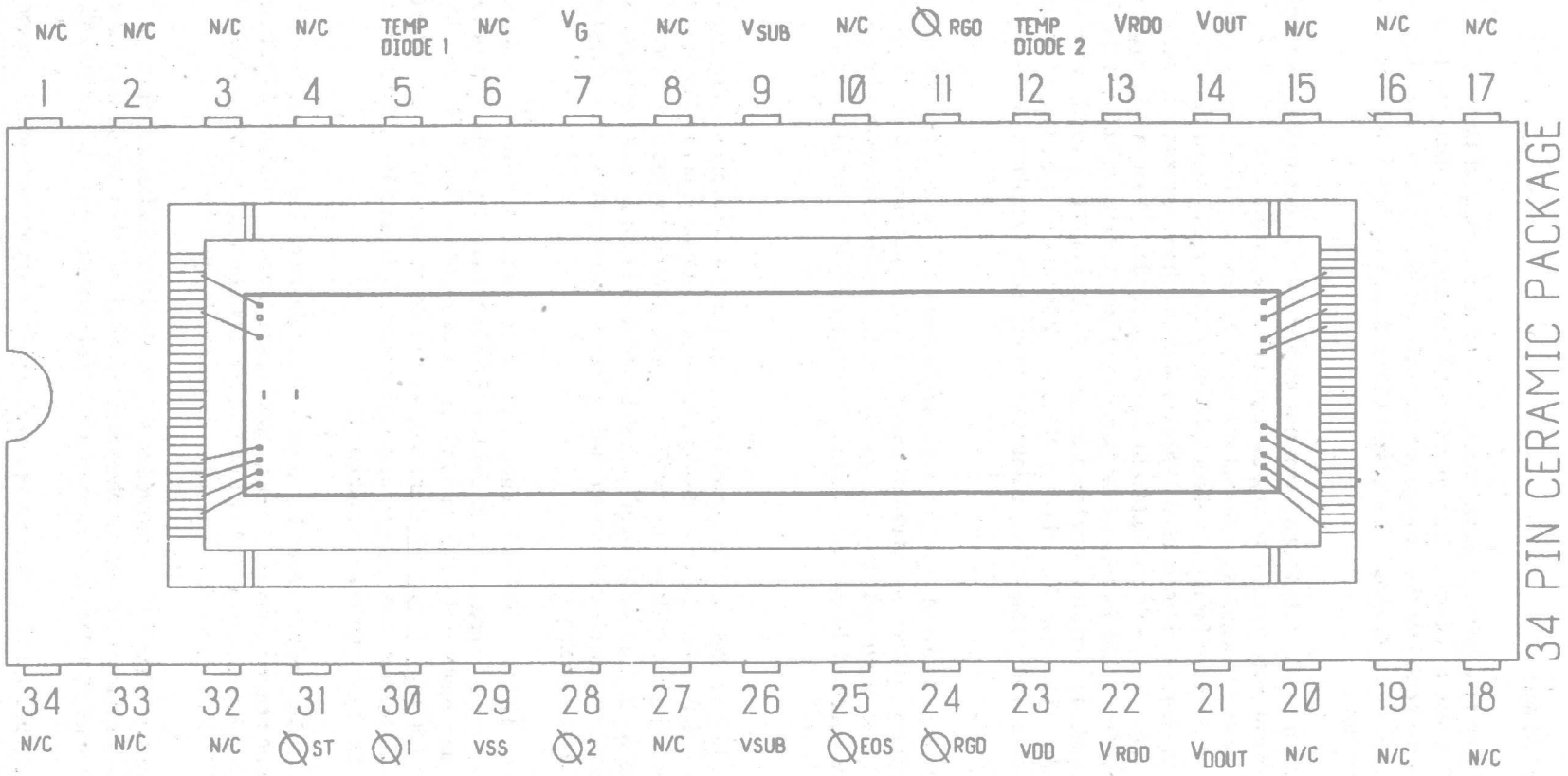

Bottom view of package, before opaque lid glued on, pins coming out of page.

Figure 1. PtSi Spectroscopic IR Linear Array Pinout.
Pixel 1 is located at left.
Temperature Diodes are located at either end of the array.

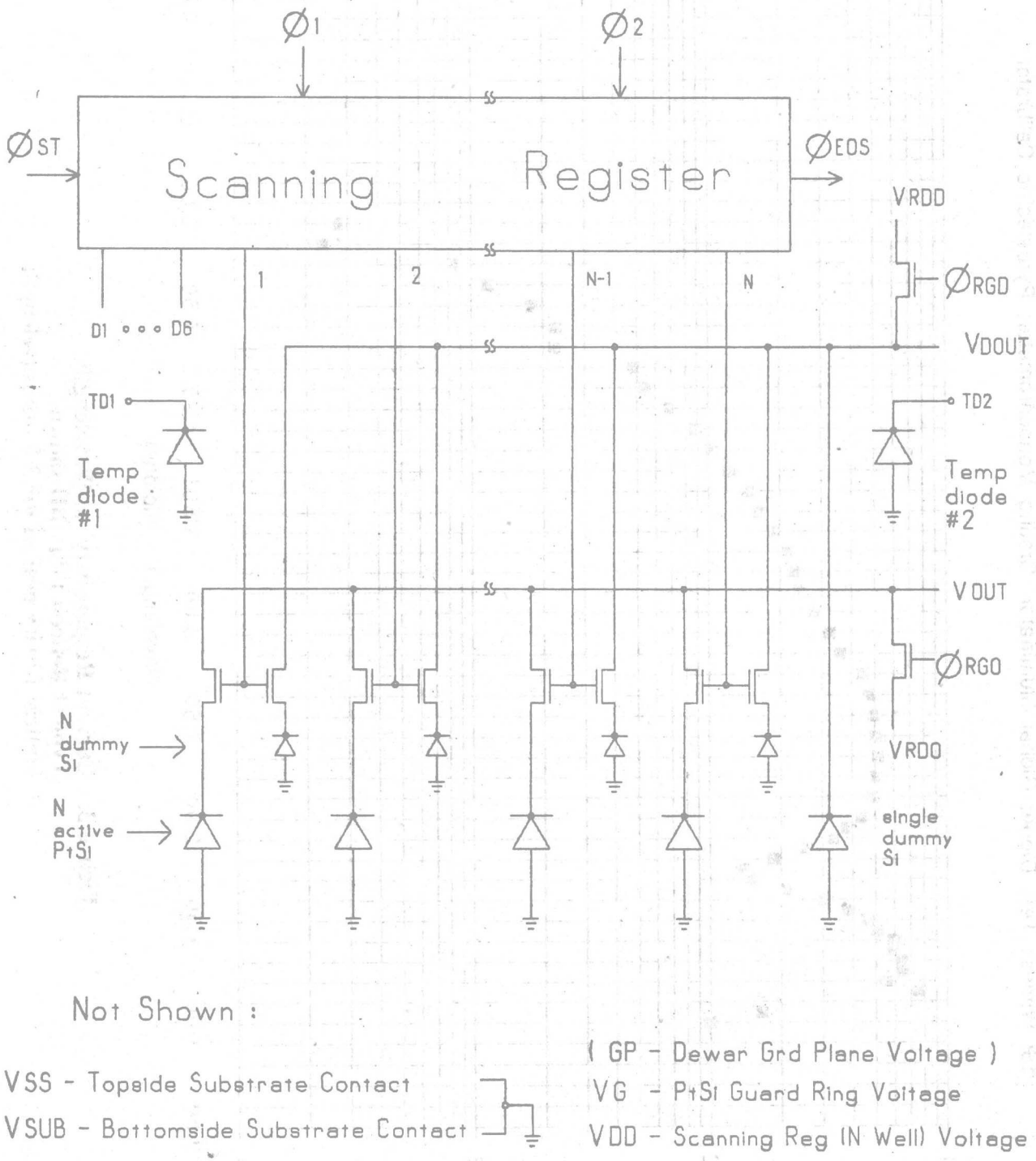

Figure 2. PtSi Spectroscopic IR Linear Array Schematic.